Proceedings of IMECE'03
2003 ASME International Mechanical Engineering Congress & Exposition
Washington, D.C., November 16-21, 2003

DRAFT **IMECE2003-41216**

CRYSTALLIZATION OF SPUTTERED NiTi FILMS

Michael J. Vestel
Lab for Ultra Small Technology Engineering and Research (LUSTER)
Berkeley Lab,
Berkeley, CA 94720 USA
email: mvestel@lbl.gov

David S. Grummon
Department of Chemical Engineering and Materials Science, Michigan State University, East Lansing, MI 48824 USA

Albert P. Pisano
Department of Mechanical Engineering,
University of California at Berkeley,
Berkeley, CA 94720 USA

ABSTRACT

Sputtered, crystalline thin films of nickel-titanium (NiTi) can display both superelastic properties and the shape memory effect, either of which may be used in films for MEMS sensors and actuators. However, direct deposition of crystalline NiTi films requires high deposition temperature and cooldown can lead to catastrophic delamination from extrinsic residual stress. To avoid delamination, especially for thick films (>5 micrometers) the amorphous form of NiTi can be sputter deposited at a low temperature, patterned and etched, released, and then crystallized to develop the proper microstructure. Here we report some results from a study of the crystallization process using differential scanning calorimetry (DSC) and transmission electron microscopy (TEM).

The minimum temperature for complete crystallization in a reasonable length of time was found to be about 400°C. Crystalline grains always nucleated first at the surface, rapidly grew laterally until impingement, and then continued to grow inward to form columnar grains as the parent amorphous phase was consumed. Surface roughness delayed the onset of surface nucleation. For very smooth surfaces, crystallization nucleated quickly, but after lateral impingement, growth inward was apparently more sluggish. Multiple DSC exotherms observed in some cases suggest that additional nucleation events may have occurred in the interior of the films.

INTRODUCTION

The shape memory (SME) and superelastic effects (SE) involve a thermally- and/or mechanically-induced solid-state, allotropic phase transformation between a ductile martensitic phase and a stiffer austenite phase. Superelasticity concerns the ability of a material to reversibly absorb large anelastic strains (3-6%) due to the reversible stress-induced transformation. The shape-memory effect refers to the ability of a material to be deformed in the low temperature martensitic condition and then revert to the original shape when heated to its high temperature, austenite phase.

Crystalline NiTi films are known to possess superelastic (SE) properties and display a robust shape memory effect (SME) [1-8] applicable where resilient mechanical response is essential, or where thermal actuation or sensing is desired. Photolithographically machined microelectromechanical systems (MEMS) may benefit from these effects for various reasons: very high work energy densities (as high as 25MJ/m^3) can be delivered, and outstanding fatigue resistance, high damping capacity can be obtained in a fully biocompatible alloy. One application of particular interest in the biomedical field is the fabrication of micro-needles [9-18] for transdermal or subdermal fluid transport [9-18], including the integration of micro-needles with silicon structures [19] in bio-MEMS assemblies.

The direct deposition of crystalline NiTi alloys onto silicon is, however, complicated by mismatched thermal expansion coefficients [20, 21]. Large tensile stresses induced when NiTi films cool can cause catastrophic delamination in films thicker than 5 to 7 microns [3]. For these thicker films this obstacle can be overcome by using low temperature deposition to obtain an amorphous phase. The amorphous film can then be lithographically etched, released from the substrate, and crystallized in an annealing step. Amorphous films have the additional advantage that HF etchants yield more precise etch profiles and smoother surfaces [22, 23]. Crystallization is therefore preferably done after micromachining operations are largely complete. Exploiting these advantages, especially in

the case of temperature-sensitive substrates, requires good understanding of the crystallization (devitrification) process in sputtered amorphous NiTi.

BACKGROUND

Moberly, *et al*. [1] confirmed that amorphous deposits crystallized to the ordered B2 (CsCl) phase and measured a crystallization enthalpy of 21.6 J/g at 490ºC in DSC experiments. Gisser, *et al*, [24] found that NiTi thin films deposited onto (100) silicon substrates at elevated temperature (460ºC) were crystalline and had [110] texture. This study showed that deposition temperatures could be lowered to 350ºC after nucleation of the crystalline phase at >460ºC. It was later shown by Hou et al. [2] that [110] texture disappeared at deposition temperatures above 425ºC.

Chen, *et al.* [25] compared the activation energies determined by Kissinger's method of sputtered amorphous $Ti_{49.93}Ni_{50.07}$ and $Ti_{49.96}Ni_{40.09}Cu_{9.95}$ films. They reported amorphous films containing Cu were thermally less stable than the nearly equiatomic NiTi film with crystalline activation energies and isochronal crystallization temperature (T_x) for a 10 K/min DSC heating rate of, respectively, 388kJ/mol and 497ºC for $Ti_{49.96}Ni_{40.09}Cu_{9.95}$ compared to 416kJ/mol and 482ºC $Ti_{49.93}Ni_{50.07}$.

Chang [8] showed that T_x at 10 K/min decreased with increasing Ti content, from 490ºC for $Ni_{52.6}Ti_{47.4}$, to 475ºC for $Ni_{49}Ti_{51}$, and observed a systematic increase of T_x with heating rate that allowed estimates for the activation energy for crystallization that ranged from 385 kJ/mol for $Ni_{49}Ti_{51}$ to 501 kJ/mol for $Ni_{52.6}Ti_{47.4}$. It was further shown that crystallization was entirely polymorphic[1]. Grummon and Zhang [26] showed that isothermal crystallization of NiTi on (100)-Si produces a transient increase in tensile film stress of approximately 180 MPa. The time for this stress to develop was analyzed as a function of the annealing temperature to give an activation energy for growth of the crystalline phase of 477 kJ/mol.

Recently, the sensitivity of microstructure to crystallization temperature was elegantly demonstrated by Kajiwara [6] in which $Ni_{48.2}Ti_{51.8}$ films, annealed at 472ºC for 1 hour, developed fine GP-zone-like precipitates that very effectively increased the critical resolved shear stress for slip. Annealing at 414ºC for 2 h maximized the strengthening effect at the expense of incomplete crystallization.

The present work was undertaken to clarify details of the crystallization process in free-standing sputtered NiTi films, and to establish critical kinetic parameters governing isothermal nucleation of the crystalline phase between 390ºC and 450ºC (below the nominal isochronal crystallization temperature). Such low temperature, post processing crystallization anneals would be favorable for post CMOS modular integration.

EXPERIMENTAL PROCEDURES

Near-equiatomic NiTi films were deposited on stainless steel (SS) and silicon substrates by DC diode magnetron sputtering. The NiTi film deposited on SS was sputtered from 75 mm diameter Ti Ni_{48} alloy targets under 3.0 mTorr of argon gas at chamber-ambient temperature (~100 °C) and a cathode power of 250 W. Ti-rich target materials were used to compensate for Ti depletion during the sputtering process. This 22 micron thick amorphous, near-equiatomic film was brittle, with a dull metallic luster, and a pronounced surface roughness inherited from the substrate finish. Large pieces were easily peeled from the substrate.

A 13 micron amorphous film was sputter-deposited on a five-inch polished (100)-silicon substrate using the similar deposition conditions. This film was tough, very smooth, and had a bright metallic luster. The metallized wafer was diced and the films delaminated by repeated thermal shock cycles between liquid nitrogen and 100°C water. X-ray diffraction confirmed that the films were amorphous.

Both films were isothermally or isochronally annealed in aluminum pans utilizing a power-compensated TA Instruments 2920 DSC under a nitrogen atmosphere. For isothermal anneals, the furnace and reference pan were equilibrated at the desired temperature, the furnace lid removed, and the sample quickly placed into the furnace just prior to recording data. This approach allowed minimal overshoot and fastest temperature equilibration. Isochronal calorimetry for determination of the dynamic crystallization temperature was performed in a method similar to Scott [27] and others [28-30] at a constant rate of 10K/min. The onset of crystallization at this heating rate for a 22μm thick amorphous film released from a SS substrate was marked by a single distinct 33J/g exotherm at 451ºC, in general agreement with previously published results [30-32]. This temperature was taken to be the dynamic crystallization temperature, T_x. Additional free-standing film specimens, detached from both Si and SS substrates, were isothermally crystallized in the calorimeter at progressively lower temperatures until no crystallization exotherm could be observed in 600 minutes.

In regard to the experimental determination of the phase fraction transformed (crystallized), $X(t)$, at time t, it has been shown [33-37] to correspond with the fractional area under the exothermal crystallization peak in a DSC thermogram, $A(t)/A_{total}$, integrated from the onset of transformation at time τ, to some later time t. The incubation period, τ, refers to the time to establish a population of critical nuclei of the crystalline phase. Integration of the peak areas, carried out using the TA Universal Analysis DSC software package (with baselines appropriately interpolated) produced sigmoidal transformation curves like the one shown in Fig. 1, from which the time for 50% ($X=½$) crystallization and the incubation period were determined. Crystalline fractions for a minimum of 100 different times were calculated. Activation energies were estimated (the plots are not shown) from a relationship of the form:

$$t_{X=½} = t_0 \exp(Q/RT) \qquad (1)$$

where t_0 is a constant, Q is the activation energy, and R is to molar gas constant, such that the slope of $\ln(t_{X=½})$ vs $1/RT$ yields Q.

[1] The latter was a significant finding from the standpoint of thin film fabrication, in the sense that it was shown that solid-state titanium supersaturation (which is virtually impossible to achieve in melt solidified alloys) was readily obtained in sputtered films, greatly expanding the range of useful compositions.

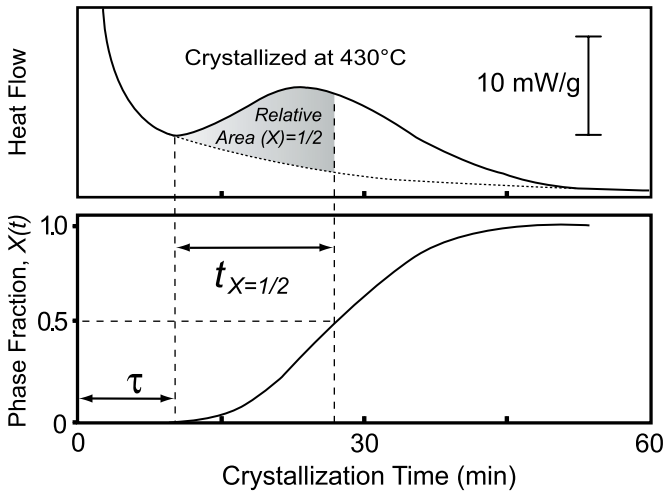

Figure 1: Typical DSC curve for an isothermal anneal. This film was released from its SS substrate and annealed at 430ºC. Also shown is the *X* vs. *t* sigmoidal type relationship illustrating the incubation time, τ (11 min.), and the time for 50% crystallization (17 min.) used to determine activation energy for crystallization.

The calorimetry data were additionally used to design isothermal annealing experiments for production of film specimens with carefully controlled partial crystallization at 420ºC. TEM observations were made on both partially and fully transformed films to study phase front morphology at various crystallization temperatures below the nominal T_x.

Transmission electron microscopy samples were prepared by the wedge method [38]. Final ion milling was done using a Fischione Instruments model 3000 ion mill with two guns tilted 12º above and below the TEM foil surface. The guns were turned on 30º before the gun was normal to the interface and turned off 30º after for times between 60-120 minutes at 5kV and between 4.0 and 5.5mA. A final cleanup step was performed at 4kV and 4.0mA using a 6º tilt with the guns turned on for the entire rotation of the sample.

Transmission electron microscopy and energy dispersive X-ray microanalysis were performed on JEOL JEM3010, Philips CM200 and JEOL JEM200CX machines at the National Center for Electron Microscopy (NCEM) [39]. .

RESULTS

NiTi Films Released from a Stainless Steel Substrate

Amorphous NiTi films released from stainless steel substrates were isothermally crystallized in the calorimeter at temperatures between 440 and 390 ºC for times as long as 600 minutes. The lowest crystallization temperature at which an exothermic peak could be easily discerned was 420ºC, as shown in Fig. 2. As the annealing temperature was lowered from 440ºC to 420ºC, the incubation time increased and the devitrification curve broadened out, as diffusion became progressively more sluggish [35, 36, 40, 41]. Annealing at 400ºC for 400 minutes and 390ºC for 600 minutes produced no identifiable crystallization exotherm.

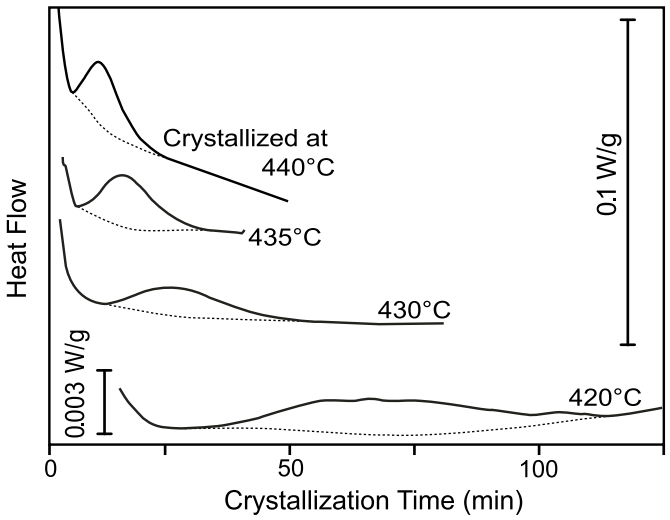

Figure 2: Isothermal DSC measurement of a 22μm amorphous equiatomic NiTi film released from a SS substrate showing broadening of crystallization peaks and increase in incubation times as the crystallization temperature was lowered. Films annealed at 400°C and 390°C showed no distinguishable exotherms.

The incubation times (τ) and times for 50% crystallization (t_x) determined from Fig. 2 are summarized in Table 1.

Table 1: Transformation times for films released from Stainless Steel

T (°C)	τ (min)	$t_{X=0.5\ ½}$(min)
420	29	37
430	11	17
435	5	10.7
440	4	6.84

The activation energy based on simple Arrhenius-law analysis of times for 50% crystallization at these various temperatures was 347 kJ/mol (83kcal/mol), within the range of previously reported values for NiTi, as well as other metallic glass systems [1, 8, 25-27, 33, 42-44]. The attempt rate (~10^{29}/s) was, however, seemingly non-physical.

Careful study of transmission micrographs of the specimen annealed at 430°C indicated that the crystalline phase had more or less simultaneously nucleated at both free surfaces. One such image of a film crystallized for 25 minutes (Fig. 2) shows a 4.7 micron deep crystalline zone at one of the two free surfaces where nucleation occurred. Nucleation and growth was followed by lateral (in-plane) grain impingement and finally columnar growth in the direction of the film-plane normal. A higher magnification image of the crystalline/amorphous interface (Fig. 3 inset) shows that the phase-front is fairly flat, i.e., that the crystalline grains are all growing at nearly the same rate as they consume the amorphous phase. The typical grain diameter in the plane of the film is approximately one micron, similar to values reported elsewhere in the literature for NiTi films devitrified from the amorphous state [4, 45, 46].

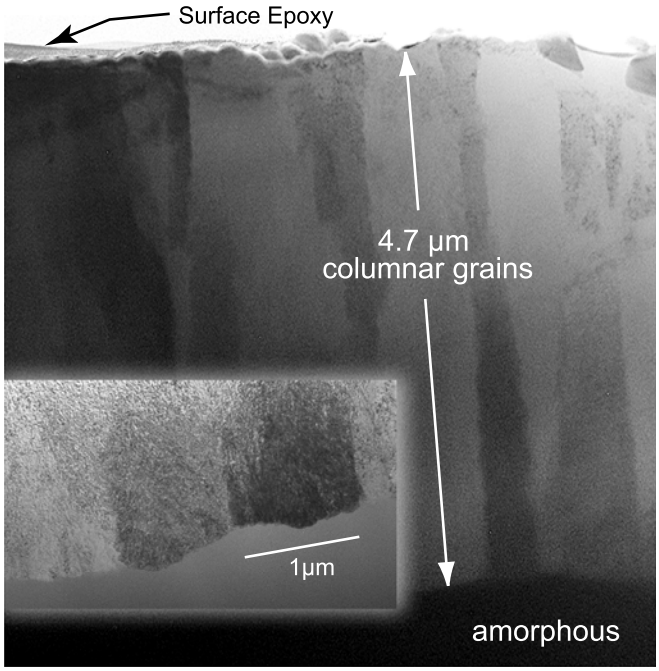

Fig. 3: TEM image of one of two free surfaces showing crystallization must have occurred at the surface, followed by grain impingement and finally by columnar growth of the grains consuming the amorphous phase. This TEM is of a sample annealed at 430ºC and quenched in liquid nitrogen after 25 minutes. Inset: Close-up of interface showing the grain size is approximately 1µm.

Analysis of the two films annealed at 430ºC, one for 80 minutes and one for 25 minutes, confirmed that the relative area under the DSC exotherm accurately corresponds to the fraction that has crystallized.

NiTi Films Released from (100) Silicon

DSC thermograms for films released from silicon are shown in Fig. 4. Note that all of the scans show evidence of multiple exothermic peaks. As was the case for films detached from SS substrates, films annealed at temperatures below 420°C did not produce a detectable exotherm during isothermal holds for up to 600 minutes. However, TEM examination indicated that films annealed at 400°C for 400 minutes were fully crystalline. A TEM micrograph of a film annealed at 390ºC for 600 minutes revealed only surface-nucleated columnar grains impinging on a remnant amorphous stratum in the center of the film. Incubation times (τ) and times to 50% crystallization (t_x) for films released from silicon are summarized in Table 2 for anneals done at 440 and 450ºC. (DSC scans at lower temperatures showed strong splitting of the exotherms, suggestive of separate nucleation regimes, which will be treated elsewhere.) The activation energy implied by these two data points is 430 kJ/mol, also with a non-physical attempt rate of > 10^{33}. Note that the incubation times, τ, are markedly shorter for the smooth-surfaces compared to the rough-surface condition.

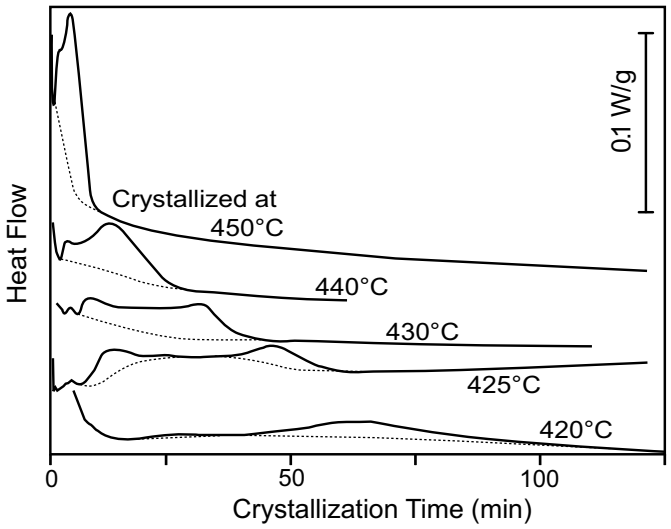

Figure 4: Isothermal anneals of freestanding NiTi released from a silicon substrate. The enclosed area represents the enthalpy of crystallization. Double crystallization peaks imply different parts of the film crystallized at different times, consistent with TEM observations of surface and interior nucleation.

Table 2: Kinetic Parameters for films released from Silicon

T (°C)	τ (min)	$t_{X=0.5\ ½}$(min)
440	1.6	10.1
450	1.1	3.7

Lamellar Microstructures

The details of the polymorphic transformation kinetics for these two example alloys remain under study, and differences in Arrhenius-law activation energies observed (with their non-physical attempt rates) may simply reflect experimental uncertainties. However, the tendency for crystallites to surface-nucleate more quickly on smooth-surface specimens compared to rough-surface films seems reasonable considering that surface diffusion probably plays a critical role in the nucleation kinetics. Although rough surfaces may present geometrically favorable heterogeneous nucleation sites, lengthened diffusion paths, and higher local curvature on a rough surface, would be inhibitory. Furthermore, the coarse scale of the roughness topography might spatially constrain the nucleation density.

The more curious result concerns the multiple peaks in the DSC spectra of the smooth surface specimens NiTi on silicon) that are evident at all temperatures in Fig. 4. They are suggestive of multiple nucleation and growth regimes operating with distinct kinetic parameters, as evidenced by the increasing interval between peaks at low temperatures. That such independently-nucleated transformation regimes do, in fact, occur in these specimens is made clear by TEM images of transverse foils made from partially-crystallized films, showing the full through-thickness structure. For rough-sufrace materials (that showed only a single DSC crystallization peak), partially crystallized materials contained three strata: two outer zones of surface-nucleated columnar grains, and an inner zone of remnant, perfectly homogenous amorphous metal. The interior interfaces appeared generally like that shown in Fig. 3. In sharp contrast, smooth-surface films, which expressed multiple crystallization exotherms, often contained as many as

five or more distinct microstructural layers, perfectly stratified in the plane of the film, with highly anisotropic polycrystalline structures having radically different single-grain aspect ratios. Relatively tall and thin columnar grains, grown from the surface, were easily identified, but additional strata of crystalline material (that had clearly nucleated in the bulk) were present. These strata generally contained wide, flat grains, indicating that crystallite growth rate was substantially higher in the lateral rather than the through-thickness direction. An example of one of these complex stratified microstructures is shown in Fig. 5. This TEM is of a film released from its silicon substrate and annealed for 120 minutes at 425ºC. The two DSC peaks shown in Fig. 4 likely correspond to the two types of microstructures seen here.

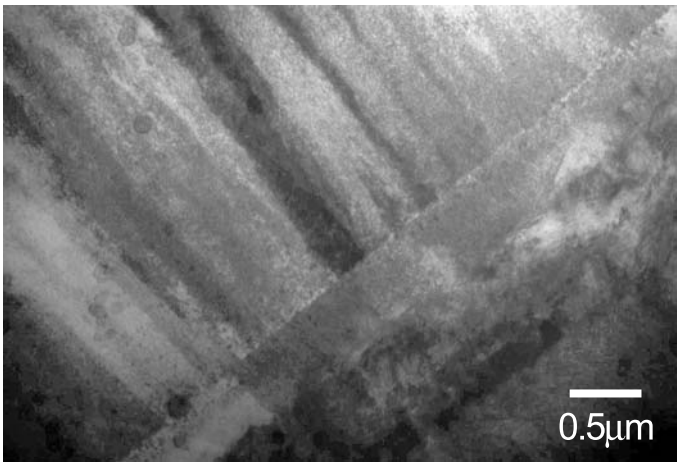

Figure 5: TEM image of interface between long, thin surface nucleated columnar grains and stratified plate shaped grains. This TEM is of a sample annealed at 425ºC for 120 minutes.

CONCLUSIONS

Low temperature, post processing crystallization anneals have been shown to successfully crystallize freestanding NiTi films. Such low annealing temperatures would be favorable for their CMOS compatibility and thus are important to the applications of MEMS structures. From this initial study of crystallization of thick, free-standing amorphous NiTi films, released from both rough stainless steel and smooth (100) silicon substrates, we additionally conclude the following:

1. Crystallization in a reasonable length of time requires annealing temperatures of at least 400^{o}C.

2. Crystallization nucleates first at free surfaces, with incubation times increasing with decreasing temperature, and with transformation rates displaying activation energies between 346 and 430 kJ/mol. Roughened surfaces appear to lengthen the nucleation phase. Nucleation occurs almost simultaneously at both free surfaces and leads to impingement of columnar grains near the center of the film when crystallization is complete. Amorphous-crystalline interfaces were found to be nominally flat.

3. Initial rapid lateral growth of surface nucleated crystallites leads to early impingement of the grains within the plane of the film, after which continued growth normal to the surface proceeded at a substantially slower rate. In-plane grain profiles were equiaxed, with a typical grain diameter of 1 micrometer, and were elongated in the film growth direction. Little dependence of grain size on annealing temperature was observed.

4. Even when surface nucleation took place rapidly, additional bulk nucleation events were found to occur that produced stratified regions of crystalline material with relatively shallow, wide grains, in sharp contrast to the aspect ratio of the surface-nucleated grains. This indicates that lateral growth rates for crystalline grains were faster than through-thickness rates, even for grains nucleated in the bulk of the film. This phenomenon leads to inhomogenous laminar microstructures that can be expected to show altered martensitic transformation behavior.

ACKNOWLEDGMENTS

The films used in this study were prepared by Thomas LaGrange and Wangyang Ni. The authors thank Professor Nitash P. Balsara and Hany Eitouni, Department of Chemistry, UC Berkeley, for use of the DSC, and Dr. Eric Stach, Dr. Tamara Radetic and Chris Nelson, Lawrence Berkeley National Laboratory, for assistance with TEM. A special thanks to Dr. Samuel Broydo for technical advice.

REFERENCES

[1] Moberly, W. J., J. D. Busch, A. D. Johnson and M. H. Berkson, 1991, "In-Situ HVEM of Crystallization of Amorphous TiNi Thin Films," presented at Phase Transformation Kinetics in Thin Films Symposium, Anaheim (CA), pp. 85-90.
[2] Hou, L. and D. S. Grummon, 1995, "Transformational superelasticity in sputtered titanium-nickel thin films," *Scripta Metallurgica et Materialia*, **33** (6), pp. 989-995.
[3] Grummon, D. S., T. LaGrange and J. Zhang, 2000, "Processing and deployment of sputtered thin films of NiTi and NiTiX alloys for biomedical and MEMs applications," presented at Proc. SMST, Alisomar (CA)
[4] Kajiwara, S., K. Ogawa, T. Kikuchi, T. Matsunaga and S. Miyazaki, 1996, "Formation of nanocrystals with an identical orientation in sputter-deposited Ti-Ni thin films," *Philosophical Magazine Letters*, **74** (6), pp. 395-404.
[5] Miyazaki, S., K. Nomura, A. Ishida and S. Kajiwara, 1997, "Recent developments in sputter-deposited Ti-Ni-base shape memory alloy thin films," presented at IVth European Symposium on Martensitic Transformations, ESOMAT '97, Enschede, Netherlands, pp. C5: 275-80.
[6] Kajiwara, S., T. Kikuchi, K. Ogawa, T. Matsunaga and S. Miyazaki, 1996, "Strengthening of Ti-Ni shape-memory films by coherent subnanometric plate precipitates," *Philosophical Magazine Letters*, **74** (3), pp. 137-44.
[7] Otsuka, K. and C. M. Wayman. 1998. *Shape Memory Materials*. Cambridge: Cambridge University Press.
[8] Chang, L. and D. S. Grummon, 1997, "Phase transformations in sputtered thin films of $Ti_x(Ni,Cu)_{1-x}$ II: Displacive transformations," *Philosophical Magazine A*

(Physics of Condensed Matter: Structure, Defects and Mechanical Properties), **76** (1), pp. 191-219.
[9] Najafi, K. and K. D. Wise, 1986, "An implantable multielectrode array with on-chip signal processing," *IEEE Journal of Solid-State Circuits*, **SC-21** (6), pp. 1035-44.
[10] Chen, J. and K. D. Wise, 1994, "A multichannel neural probe for selective chemical delivery at the cellular level," presented at Solid-State Sensor and Actuator Workshop, Hilton Head Island (SC), pp. 256-259.
[11] Lin, L. and A. P. Pisano, 1999, "Silicon-processed microneedles," *Journal of Microelectromechanical Systems*, **8** (1), pp. 78-84.
[12] Talbot, N. H. and A. P. Pisano, 1998, "Polymolding: two wafer polysilicon micromolding of closed-flow passages for microneedles and microfluidic devices," presented at Solid-State Sensor and Actuator Workshop, Hilton Head Island (SC), pp. 265-8.
[13] Brazzle, J., D. Bartholomeusz, R. Davies, J. Andrade, R. A. van Wagenen and A. B. Frazier, 2000, "Active microneedles with integrated functionality," presented at Solid-State Sensor and Actuator Workshop, Hilton Head Island (SC), pp. 199-202.
[14] Papautsky, I., J. Brazzle, H. Swerdlow and A. B. Frazier, 1998, "A low-temperature IC-compatible process for fabricating surface-micromachined metallic microchannels," *Journal of Microelectromechanical Systems*, **7** (2), pp. 267-73.
[15] Papautsky, I., A. B. Frazier and H. Swerdlow, 1997, "A low-temperature IC-compatible process for fabricating surface-micromachined metallic microchannels," presented at Tenth Annual International Workshop on MEMS, Nagoya, Japan, pp. 317-22.
[16] Brazzle, J. D., I. Papautsky and A. B. Frazier, 1998, "Fluid-coupled hollow metallic micromachined needle arrays," presented at Microfluidic Devices and Systems, Santa Clara (CA), pp. 116-24.
[17] Papautsky, I., J. Brazzle, T. Ameel and A. Bruno Frazier, 1998, "Laminar fluid behavior in microchannels using micropolar fluid theory," presented at IEEE Eleventh Annual International Workshop on MEMS, Heidelberg, Germany, pp. 101-8.
[18] Henry, S., D. V. McAllister, M. G. Allen and M. R. Prausnitz, 1998, "Micromachined needles for the transdermal delivery of drugs," presented at Eleventh Annual International Workshop on MEMS, Heidelberg, Germany, pp. 494-8.
[19] Franke, A. E., 2000, "Polycrystalline silicon-germanium films for integrated microsystems," Ph.D. thesis, University of California at Berkeley, Berkeley, CA.
[20] Haji, L., P. Joubert, M. Guendouz, N. Duhamel and B. Loisel, 1991, "Substrate effects on the kinetics of solid phase crystallization in α-Si," presented at Phase Transformation Kinetics in Thin Films Symposium, Anaheim, CA, USA, pp. 177-82.
[21] Kim, J. J., P. Moine and D. A. Stevenson, 1986, "Crystallization behavior of amorphous Ni-Ti alloys prepared by sputter deposition," *Scripta Metallurgica*, **20** (2), pp. 243-8.
[22] Makino, E., T. Mitsuya and T. Shibata, 2000, "Micromachining of TiNi shape memory thin film for fabrication of micropump," *Sensors and Actuators A (Physical)*, **A79** (3), pp. 251-9.
[23] Guifu, D., Y. Aibin, Z. Xiaolin, X. Dong, C. Bingchu and S. Tianhui, 1999, "Patterning of nickel-titanium SMA films with chemical etching by a novel multicomponent etchant," presented at Device and Process Technologies for MEMS and Microelectronics, Gold Coast, Qld., Australia, pp. 340-5.
[24] Gisser, K. R. C., J. D. Busch, A. D. Johnson and A. B. Ellis, 1992, "Oriented nickel-titanium shape memory alloy films prepared by annealing during deposition," *Applied Physics Letters*, **61** (14), pp. 1632-4.
[25] Chen, J. Z. and S. K. Wu, 2001, "Crystallization temperature and activation energy of rf-sputtered near-equiatomic TiNi and Ti/sub 50/Ni/sub 40/Cu/sub 10/ thin films," *Journal of Non-Crystalline Solids*, **288** (1-3), pp. 159-65.
[26] Grummon, D. S. and J. Zhang, 2001, "Stress in sputtered films of near-equiatomic TiNiX on (100) Si: intrinsic and extrinsic stresses and their modification by thermally activated mechanisms," *Physica Status Solidi A*, **186** (1), pp. 17-39.
[27] Scott, M. G. and P. Ramachandrarao, 1977, "The Kinetics of Crystallization of an Fe-P-C Glass," *Materials Science and Engineering*, **29** (2), pp. 137-144.
[28] Marshall, A. F., R. G. Walmsley and D. A. Stevenson, 1984, "Crystallization of an amorphous $Cu_{88}Zr_{20}$ alloy prepared by magnetron sputter deposition," *Materials Science and Engineering*, **63** pp. 215-227.
[29] Makifuchi, Y., Y. Terunuma and M. Nagumo, 1997, "Structural relaxation in amorphous Ni-Ti alloys prepared by mechanical alloying," *Materials Science and Engineering*, **A226-228** pp. 312-316.
[30] Busch, J. D., A. D. Johnson, C. H. Lee and D. A. Stevenson, 1990, "Shape-memory properties in Ni-Ti sputter-deposited film," *Journal of Applied Physics*, **68** (12), pp. 6224-6228.
[31] Chang, L. and D. S. Grummon, 1997, "Structure evolution in sputtered thin films of $Ti_x(Ni,Cu)_{1-x}$. I. Diffusive transformations.," *Philosophical Magazine A (Physics of Condensed Matter: Structure, Defects and Mechanical Properties)*, **76** (1), pp. 163-89.
[32] Kajiwara, S., K. Ogawa, T. Kikuchi, T. Matsunaga and S. Miyazaki, 1996, "Unique crystallization process in sputter-deposited Ti-Ni shape memory films," presented at Ninth International Conference on Rapidly Quenched and Metastable Materials, Bratislava, Slovakia, pp. 53-5.
[33] Scott, M. G., 1978, "The crystallization kinetics of Fe-Ni based metallic glasses," *Journal of Materials Science*, **13** (2), pp. 291-6.
[34] Scott, M. G. and P. Ramachandrarao, 1977, "The kinetics of crystallisation of an Fe-P-C glass," *Material Science and Engineering*, **29** (2), pp. 137-44.
[35] Greer, A. L., 1985, "Crystal Nucleation and Growth in Metallic Liquids and Glasses," presented at Acta-Scripta metallurgica Proceedings Series, New York, pp. 94-107.
[36] Luborsky, F. E. 1983. *Amorphous metallic alloys*. London; Boston: Butterworths.
[37] Fujita, H., M. Komatsu, T. Sakata and N. Fujita, 1996, "Nucleation of crystals in amorphous materials," *Materials Transactions, JIM*, **37** (7), pp. 1350-5.
[38] Phelps, J. M., 1998, "Cross-section sample preparation of a free-standing thin-film coupon for transmission electron

microscopy analysis," *Microscopy and Microanalysis*, **4** (2), pp. 128-32.
[39] http://ncem.lbl.gov/frames/center.htm.
[40] Shimomura, K., P. H. Shingu and R. Ozaki, 1980, "The morphology of alpha -Fe crystals which grow in the amorphous $Fe_{80}(C_{1-x}B_x)_{20}$ alloys," *Journal of Materials Science*, **15** (5), pp. 1175-82.
[41] Cahn, R. W. and P. Haasen. 1983. *Physical metallurgy*. 3rd ed. Amsterdam; New York: North-Holland Physics Pub., Elsevier Science Pub. Co.
[42] Scott, M. G., 1978, "Thermal stability and crystallisation of metallic glasses," presented at Rapidly Quenched Metals III, Brighton, UK, pp. 198-213.
[43] Scott, M. G. and T. Watanabe, 1979, "Crystallisation of some metallic glasses," presented at Spring Residential Conference, York, UK, pp. III/36-8.
[44] Thompson, C. V., A. L. Greer and F. Spaepen, 1983, "Crystal nucleation in amorphous (Au/sub 100-y/Cu/sub y/)/sub 77/Si/sub 9/Ge/sub 14/ alloys," *Acta Metallurgica*, **31** (11), pp. 1883-94.
[45] Miyazaki, S. and A. Ishida, 1999, "Martensitic transformation and shape memory behavior in sputter-deposited TiNi-base thin films," *Materials Science and Engineering*, **A273-275** pp. 106-133.
[46] Chang, L. and D. S. Grummon, 1992, "Orthorhombic Martensite, Intermetallic Precipitates and Retained Austenite in Ti-Rich Ti(Ni+Cu) Sputtered Thin Films," presented at Materials Research Society Symposium, pp. 141-146.

